

# CONFIGURATION ANALYSIS OF HYBRID METAL BI-STABLE COMPOSITES

Xiangwei Guo<sup>1\*</sup>, Na Dong<sup>2</sup> and Fuhong Dai<sup>1</sup>

<sup>1</sup>National Key Laboratory of Science and Technology on Advanced Composites in Special Environment, Harbin Institute of Technology, Harbin, 150000, China

<sup>2</sup>Harbin Institute of Pharmaceutical Sciences, ZBD Pharmaceutical, Harbin, 150000, China

\*Corresponding author: xiangweig@foxmail.com

**Keywords:** Bistable composites, Finite elements, Metal mixing, Strain energy

## ABSTRACT

The bi-stable cylindrical shell is a thin-walled composite structure with a specific angle layup, which has two stable configurations and can maintain the unfolded state and the curled state without external constraints. This structure has the advantages of a simple curling storage device, a reliable unfolding process, and high storage efficiency, and has great application potential in space-deployable structures. In this paper, based on bi-stable composite materials, a method is proposed to change the deformation shape of the structure by mixing metals, to adjust the deformation characteristics of the structure to meet the needs of practical applications. The addition of metal layers to a bistable composite structure can alter the conformational curvature and also achieve the need for electrical and thermal conductivity. Here the mechanical properties of the mixed-metal bistable structure are simulated and analyzed by the finite element method. The results of this paper show that the addition of metals in different positions of the composite has a great influence on the two stable forms of the bi-stable structure.

## 1 INTRODUCTION

With the development of electronic information and communication systems, designing integrated antenna structures with multiple electromagnetic functions is an issue that needs to be solved for future aircraft and satellites[1]. Among them, the surface-antenna-structure (SAS) and composite smart structure (CCS) were designed to accomplish multi-functional and intelligent structures [2, 3]. This structure has been studied by integrating conductive materials into the composite structure, in which the integrated structure functions together and has well mechanical and electromagnetic properties[4]. With the rapid development of advanced composite materials, they are widely used in various scenarios due to the lightweight, high specific strength, and high specific stiffness of these reinforced matrix composites[5]. It is required in many fields to develop intelligent structures with integrated structure and function by using composite materials[6-7]. The bistable composite structure was discovered in the 1980s[8]. In the experiment of laminating glass fiber around a cylindrical mold, it was observed that the cylindrical shell with initial curvature has two stable configurations after curing[9]. Subsequently, researchers carried out theoretical models to predict the structure, and the existing beam model, shell model, two-parameter model, and other models were better predicted in the shallow shell and short shell model[10]. In any stable state, this structure can maintain its stable state without continuous input of energy and has the characteristics of adapting to large deformation[11]. Under the application of external loads, the bistable structure can freely switch to different structural forms by snap-through and snap-back in two stable states, and each stable state has a certain bearing capacity[12]. The large deformation feature of the bistable structure has been used as the deployment mechanism of the solar sail, which has the supremacies of high storage ratio and light weight[13]. The two deformation phenomena of the bistable structure, similar to a hinge structure with a one-dimensional degree of freedom, can achieve frictionless bending and self-locking morphology[14].

This paper presents a comprehensive mechanical analysis of bistable composite cylindrical shells mixed with metals at different locations. The effect of mixing different fibrous materials in the alignment properties is also analyzed.

## 2 MATERIALS

The schematic of the bistable composite is illustrated in Fig. 1, where Fig. 1(a) shows the configuration A shape, and Fig. 1(b) is configuration B. Configuration A and B are thin-walled cylindrical shells. The initial shape is a flat composite structure composed of fiber and epoxy resin. Based on the initial flat shape, the plate structure is bent and deformed to one side to form configuration A in Fig. 1(a). By bending configuration A in the  $x$ -axis direction, the structure is deformed to the configuration B state. Configuration B is a small size with a high storage ratio that can be maintained in this form without external force. Meanwhile, the structure can be deformed to the steady state A shape by applying an external force to the steady state B that stretches both sides of the  $z$ -axis. And steady states A and B can be repeatedly converted to each other.

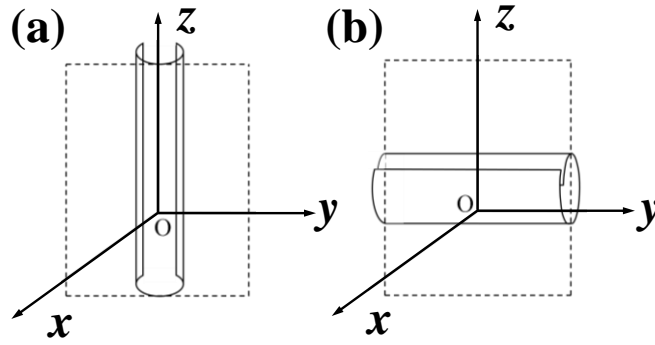


**Fig. 1.** Bistable composites: (a) Configuration A; (b) Configuration B.

The bistable composite is composed of resin, fibers, and copper foil. The three materials are integrally cured to form a bistable composite tube. In this study, the bistable composite is made of carbon fiber and glass fiber, respectively. The matrix term is using thermosetting epoxy resin. The metal layer acts as an adjustable part of the structural form. Fiber and epoxy resin will serve as the base layer of the structure responsible for deformation and reconfiguration.

## 3 MECHANICAL BEHAVIOR

### 3.1 Finite element models

Considering that the bistable composite is composed of multiple materials, its configuration prediction will be very complicated. To investigate the reconfigurable mechanism and conformational prediction, finite element method simulations were used. Here, the constitutive analysis of the bistable composite will be performed using the commercial software ABAQUS finite element method. The specific material properties are shown in Table 1.

**Table 1.** Elastic and thermal properties of CFRP, GFRP, and copper

Description	CFRP	GFRP	Copper
0°/90° Elastic modulus(GPa)	54.5	43.1	110
Shear elastic modulus(GPa)	3.07	4.3	41.7
Poisson's ratio	0.06	0.126	0.32
Thermal expansion coefficient( $10^{-6}/^{\circ}\text{C}$ )	4.16	12.5	17.7

The finite element simulation analysis process is divided into two steps, as illustrated in Fig. 2. This procedure was analyzed in ABAQUS software using implicit analysis with S4R shell cells to simulate the laminate and metal layers. The simulated laminate is [C/C/Cu] in Fig. 2. As shown in Fig. 2(a), the first step is to transform state A to state B to realize the reconfiguration of structure stowage. First, the boundary condition of the structure is set to be fixed for the centrosymmetric point of state A. Then, a bending moment is applied on both sides of the open shell to bend the two ends of the structure inwardly.

When the structure completes the snap-through, the external loads are released. The structure then shrinks to state B without external force, which is a multi-turn cylindrical shape. As shown in Fig. 2(b), the second step is to realize the snap-back from state B to state A, which is from the retracted state to the deployed state. First, the center point of the restrained laminate is maintained and a bending moment is applied to the open edge of the stowed cylindrical shell on both sides. Remove the moment when the state is about to change. Then the shell is free to deform to state A, which is the same as the initial state A. During the whole snap-through and snap-back processes, configurations A and B are both cylindrical shapes. To automate the different states, mechanical and intelligent structures can be used for the drive.

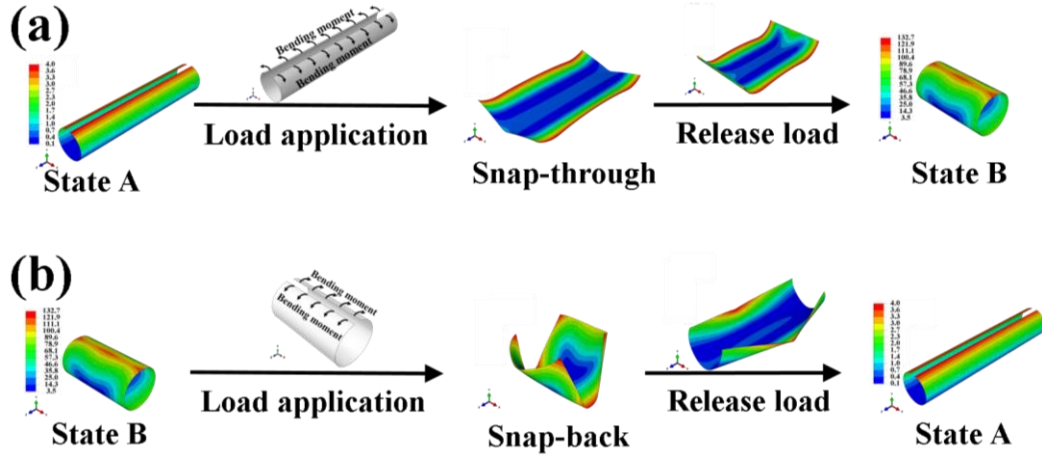


**Fig. 2.** Simulated snap-through and snap-back processes: (a) Step 1, snap-through from state A to B; (b) Step 2, snap-back from state B to A.

### 3.2 Strain energy

In this paper, six kinds of layups are designed to study the mechanical performance of the bistable composite. It shows the layup schematic of six specimens with the same fiber angle of  $45^\circ$ , the difference is that the metal is mixed in different positions of CFRP or GFRP as illustrated in Fig. 3. The metal is attached to the inner, middle, and outer sides of the carbon fiber composite for simulation. The composite was also changed to glass fiber to compare its structure with the carbon fiber material and the change in strain energy. The material layup is expressed from the inside to the outside, such as [C/C/Cu], which indicates two layers of carbon fiber composite (CFRP) inside and one layer of copper outside.

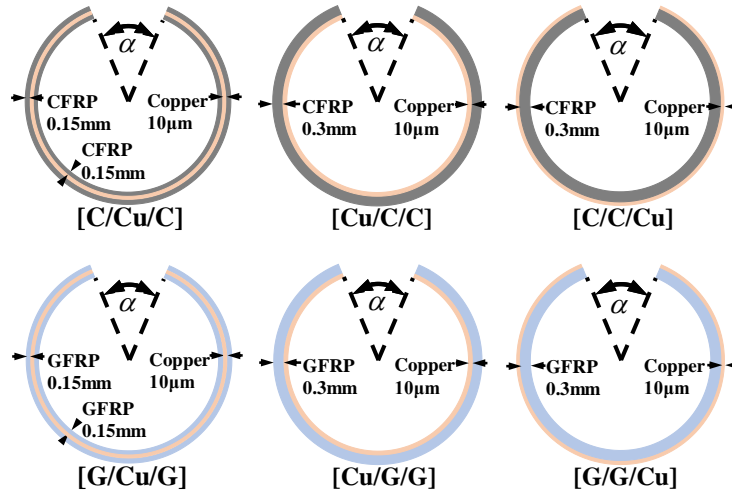


**Fig. 3.** Layup diagram of 6 specimens.

The total elastic strain of the structure is given by Equation (1) and the strain is divided along the entire area to give the bistable structural strain energy of Equation (2). Solving this equation gives the strain energy curve for the structure under two conformational transitions.

$$\begin{bmatrix} \varepsilon_x \\ \varepsilon_y \\ \varepsilon_z \end{bmatrix} = \begin{bmatrix} \varepsilon_x^0 \\ \varepsilon_y^0 \\ \varepsilon_z^0 \end{bmatrix} + z \begin{bmatrix} k_x \\ k_y \\ k_z \end{bmatrix} \quad (1)$$

$$\Pi = \int_{-L_y/2}^{L_y/2} \int_{-L_y/2}^{L_y/2} \left( \frac{1}{2} \begin{bmatrix} \varepsilon^0 \end{bmatrix}^T \begin{bmatrix} A & B \\ C & D \end{bmatrix} \begin{bmatrix} \varepsilon^0 \\ k \end{bmatrix} \right) dx dy \quad (2)$$

The simulated strain energy trends of the transition are shown in Fig. 4. After the initial state is solidified the hybrid composite enters state A. The simulated state A has an  $\alpha$  angle of  $10^\circ$ . State A rises to the first energy barrier under the action of an external force and snap-through to state B. The strain energy of state B is at a higher level and rises into the second energy barrier with a smaller external force and returns to state A with a snap-back. The strain energy of state B is greater than that of state A. It also shows that it is easy to move from the stowed state to the unfolded state because the energy is released in this process. If the energy provided by the external force is below the energy barrier, snap-through and snap-back will not occur. The trend of strain energy is similar for the 6 specimens. The copper foil laying inside the carbon fiber shell corresponds to the largest energy barrier, which means snap-through and snap-back are the hardest to happen. Whereas copper foil inside the carbon fiber has the smallest energy barrier, and it is the easiest to achieve snap-through and snap-back. But the energy barrier of carbon fiber layup is different, and snap-through energy is greater than snap-back. This indicates that the bistable tube is easier from storage to the unfolding process. The energy barrier of the glass fiber laminates in Fig. 4 is all smaller than those of the carbon fiber laminates. The main reason is that the glass fiber stiffness is less than the carbon fiber and the force applied to the glass fiber laminate is much smaller. The same rule as for the carbon fiber laminate is that the metal has the highest strain energy on the inner side. However, the snap-through and snap-back energy barriers of glass fiber are almost the same, indicating that the two states are equally difficult to switch with each other. And snap-back is longer than the snap-through process from the energy barrier diagram.

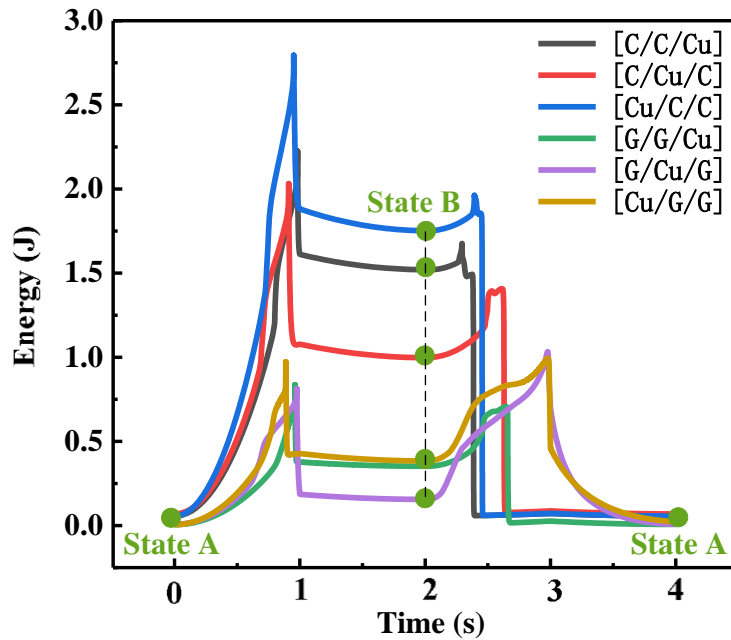


Fig. 4. Strain energy of 6 specimens.

## 4 CONCLUSIONS

In this study, a deployable and stowable structure based on a morphing bistable composite tube was described. The two conformational transition processes of the bistable structure were simulated, and the snap-through and snap-back phenomenon occur when the external force broke the energy barrier. The two states can keep the shape stable without external force in the expanded and stowed state due to the two energy wells. Six bistable composite specimens were designed, and simulated to demonstrate the effects of different fiber materials and different layups on the configuration and structure performance. The proposed metal hybrid composite tube was lightweight, deformable as well as miniaturized, providing a potential application in morphing structures.

## ACKNOWLEDGEMENTS

This work was supported by the Laboratory of Science and Technology on Advanced Composites in Special Environments.

## REFERENCES

- [1] C. Barile, C. Casavola, F. De Cillis, Mechanical comparison of new composite materials for aerospace applications, *Composites Part B: Engineering* 162 (2019) 122-128. (doi: [10.1016/j.compositesb.2018.10.101](https://doi.org/10.1016/j.compositesb.2018.10.101)).
- [2] C.K. Kim, L.M. Lee, H.C. Park, W. Hwang, W.S. Park, Impact damage and antenna performance of conformal load-bearing antenna structures, *Smart Materials and Structures* 12(5) (2003) 672-679. (doi: [10.1088/0964-1726/12/5/302](https://doi.org/10.1088/0964-1726/12/5/302)).
- [3] C. You, M.M. Tentzeris, W. Hwang, Multilayer Effects on Microstrip Antennas for Their Integration With Mechanical Structures, *Ieee T Antenn Propag* 55(4) (2007) 1051-1058. (doi: [10.1109/TAP.2007.893401](https://doi.org/10.1109/TAP.2007.893401)).
- [4] F. Xu, K. Zhang, Y. Qiu, Light-weight, high-gain three-dimensional textile structural composite antenna, *Composites Part B: Engineering* 185 (2020) 107781. (doi: [10.1016/j.compositesb.2020.107781](https://doi.org/10.1016/j.compositesb.2020.107781)).
- [5] R. Hsissou, R. Seghiri, Z. Benzekri, M. Hilali, M. Rafik, A. Elharfi, Polymer composite materials: A comprehensive review, *Composite Structures* 262 (2021) 113640. (doi: [10.1016/j.compstruct.2021.113640](https://doi.org/10.1016/j.compstruct.2021.113640)).
- [6] J. Raghavan, T. Bartkiewicz, S. Boyko, M. Kupriyanov, N. Rajapakse, B. Yu, Damping, tensile, and impact properties of superelastic shape memory alloy (SMA) fiber-reinforced polymer composites, *Composites Part B: Engineering* 41(3) (2010) 214-222. (doi: [10.1016/j.compositesb.2009.10.009](https://doi.org/10.1016/j.compositesb.2009.10.009)).
- [7] Liang F, Lin S, Guo X, et al. A Printed UWB Monopole Antenna Based on Bistable Composite Laminates[C]//2022 IEEE Microwaves, Antennas, and Propagation Conference (MAPCON). IEEE, 2022: 2055-2058. (doi: [10.1109/MAPCON56011.2022.10047726](https://doi.org/10.1109/MAPCON56011.2022.10047726)).
- [8] M.W. Hyer, Some Observations on the Cured Shape of Thin Unsymmetric Laminates, *Journal of Composite Materials* 15(2) (1981) 175-194. (doi: [10.1177/002199838101500207](https://doi.org/10.1177/002199838101500207)).
- [9] A. Daton-Lovett, Q. Compton-Bishop, R. Curry, Deployable structures using bistable reeled composites, *Proceedings of SPIE - The International Society for Optical Engineering* (2000). (doi: [10.1117/12.388250](https://doi.org/10.1117/12.388250)).
- [10] L. Yang, H. Tan, Z. Cao, Modeling and analysis of the ploy region of bistable composite cylindrical shells, *Composite Structures* 192 (2018) 347-354. (doi: [10.1016/j.compstruct.2018.02.085](https://doi.org/10.1016/j.compstruct.2018.02.085)).
- [11] Z. Zhang, G. Ye, H. Wu, J. Yang, S. Kitipornchai, G. Chai, Bistable behaviour and microstructure characterization of carbon fiber/epoxy resin anti-symmetric laminated cylindrical shell after thermal exposure, *Composites Science and Technology* 138 (2017) 91-97. (doi: [10.1016/j.compscitech.2016.11.019](https://doi.org/10.1016/j.compscitech.2016.11.019)).

- [12] B. Wang, K.A. Seffen, S.D. Guest, T.-L. Lee, S. Huang, S. Luo, J. Mi, In-situ multiscale shear failure of a bistable composite tape-spring, *Composites Science and Technology* 200 (2020) 108348. (doi: [10.1016/j.compscitech.2020.108348](https://doi.org/10.1016/j.compscitech.2020.108348)).
- [13] S.K. Jeon, T.W. Murphey, Design and analysis of a meter-class CubeSat boom with a motor-less deployment by bi-stable tape springs, *Aiaa/asme/asce/ahs/asc Structures, Structural Dynamics & Materials Conference* (2011). (doi: [doi/10.2514/6.2011-1731](https://doi.org/10.2514/6.2011-1731)).
- [14] V.S.C. Chillara, M.J. Dapino, Mechanically-prestressed bistable composite laminates with weakly coupled equilibrium shapes, *Composites Part B: Engineering* 111 (2017) 251-260. (doi: [10.1016/j.compositesb.2016.12.011](https://doi.org/10.1016/j.compositesb.2016.12.011)).